An Experimental Assessment of Modulation Methods for Drive Trains Used In Electric Vehicles

Eleftherios Kontodinas*, Andreas Kraemer†, Hans-Dieter Endres†, Sebastian Wendel†, Petros Karamanakos*, and Joao Bonifacio†

*Faculty of Information Technology and Communication Sciences, Tampere University, 33101 Tampere, Finland

Email: *eleftherios.kontodinas@tuni.fi, p.karamanakos@ieee.org

†ZF Friedrichshafen AG, 97424 Schweinfurt, Germany

Email: †andreas.kraemer@zf.com, hans-dieter.endres@zf.com, sebastian.wendel@zf.com, joao.bonifacio@zf.com

***Abstract*—As the number of electric automotive vehicles is rapidly growing, the need for higher efficiency and system-friendly operation of the drive train becomes more relevant and urgent. In this paper, the synchronous modulation schemes of selective harmonic elimination (SHE) and optimized pulse patterns (OPPs) are described and their performance benefits for drives used in automotive industry are highlighted. The presented experimental results based on an industrial drive demonstrate that OPPs achieve superior performance in terms of current distortions, system efficiency, and dc-link current ripple compared with conventional asynchronous space vector modulation (SVM).**

I. Introduction

Throughout the development of electric automotive vehicle technology, various electrical machines have been utilized. Since in propulsion applications the drive train is used over the entire speed/torque capabilities, it has to be designed such that high acceleration/deceleration rates (i.e., high torque output over the whole speed range) and efficient cruising at higher speeds are achieved. This indicates the need for machines with high torque density and efficiency at all speeds. Given this, the most commonly used machines in the applications of interest are the three-phase permanent magnet synchronous machines (PMSMs) [1].

The control system is an essential part of the drive train and has a crucial role in operating it at its full potential. The control methods most commonly used for commercial electric vehicles are the direct torque control (DTC) and field oriented control (FOC) in conjunction with asynchronous pulse width modulation (PWM) techniques [2]. Nevertheless, to produce currents with higher quality, and thus improve the efficiency of the drive train, more sophisticated modulation methods are required, such as programmed PWM methods [3], [4]. Such methods—also referred to as synchronous modulation—include selective harmonic elimination (SHE) and optimized pulse patterns (OPPs).

The first programmed PWM method, namely SHE, is an offline optimization technique that eliminates selected voltage harmonics regardless of the load characteristics [5]–[7]. The SHE problem is based on the Fourier decomposition of the switched output voltage waveform of the inverter. The problem of finding the switching angles, i.e., the pulse pattern, that eliminate the selected harmonics is written as a system of nonlinear, transcendental, trigonometric equations. A property of this system is that it exhibits multiple solutions, the number of which increases with the number of harmonics to be eliminated. As a result, the to-be-solved system is more complicated and thus more difficult to solve; it may even become unsolvable.

As for the OPPs, these are pulse patterns that can produce the minimum harmonic distortion at a given switching frequency [8]. Similar to SHE, the pulse patterns are calculated in an offline procedure assuming steady-state conditions. However, as opposed to SHE, to compute OPPs, an optimization problem is formulated where the objective function captures the current distortions. By minimizing this objective function subject to constraints on the fundamental voltage component and the order of the switching angles, an optimal set of switching angles is derived for every modulation index, which is typically unique [9].

The aforementioned potential efficiency improvements motivated GE to adopt high-performance PWM strategies in the 1980s for its high-power traction drives used in railway applications [10]. These techniques were a combination of asynchronous modulation at low speeds and synchronous modulation—in the form of SHE—at higher speeds. For the same applications, SIEMENS also adopted synchronous modulation, with the difference that OPPs were used instead [11].

Even though these techniques were developed mainly for induction machines, the apparent advantages of programmed PWM methods recently stimulated the interest of the automotive industry towards similar hybrid modulation techniques for low-voltage interior PMSM (IPMSM) drives with high operating point dependent magnetic anisotropy. As such drive systems are operating at high fundamental frequency—with the switching frequency being in the lower kilohertz range—synchronous modulation schemes can be employed to avoid sub-harmonic content and keep the switching as well as machine losses low. Moreover, programmed PWM methods become even more relevant as the switching-to-fundamental frequency ratio becomes smaller, as there are only a few switching instants per fundamental period. This implies that small changes in the applied voltage (i.e., pulse pattern) may have considerable impact on the harmonic distortion of the machine currents. Therefore, it is favorable to use high-

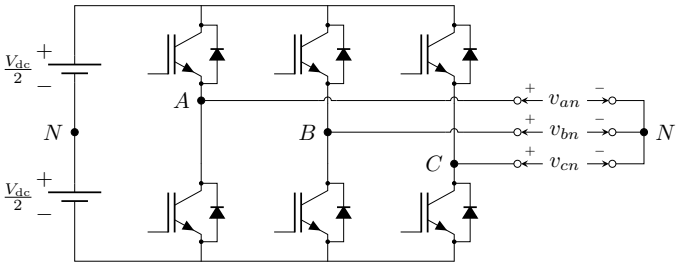

Fig. 1: Two-level voltage voltage source inverter.

performance PWM methods which can produce high-quality currents.

In this direction, Silicon Mobility adopted an adaptive FOC-based controller that uses space vector modulation (SVM) at lower speeds and OPPs at higher speeds [12]. The pulse patterns are optimized based on multiple criteria, such as current distortions, torque ripple, and noise vibrations. Similarly, DENSO employed a combination of modulation strategies for different operating points of the drive train [13]. The modulation scheme starts with carrier-based PWM (CB-PWM) at lower speeds, discontinuous PWM (DPWM) in the medium speed range, while OPPs are used at the upper end of the speed range and up to six-step modulation. Similarly, BMW also utilized asynchronous SVM and OPPs [14].

Considering the above, this paper compares three modulation techniques for an IPMSM drive train used in electric automotive vehicles. These methods, namely asynchronous PWM, SHE, and OPPs, are experimentally assessed under several operating points. In doing so, the benefits of synchronous PWM, and especially OPPs, are clearly demonstrated in terms of current distortions, system efficiency, and ripple of the dc-link current.

II. Synchronous Modulation

The industrial drive system considered in this work consists of a two-level inverter and an IPMSM. Assuming a dc-link voltage $V_{\rm dc}$, the inverter (see Fig. 1) produces a switched voltage on each phase $x \in \{a, b, c\}$ that assumes two values, namely $V_{\rm dc}/2$ when the corresponding switch position is $u_x = 1$, and $-V_{\rm dc}/2$ when $u_x = -1$. Considering that the waveform $u \equiv u_a$ has a period of 2π, then the number of pulses in one period is $q = f_{\rm sw}/f_1 \in \mathbb{N}^+$, where $f_{\rm sw}$ and f_1 are the switching and the fundamental frequency, respectively.

In synchronous modulation, it is common practice to impose quarter- and half-wave symmetry (QaHWS) on the switched waveform $u(\theta)\,\forall\theta \in [0, 2\pi]$, i.e.,

$$u(\theta) = -u(\pi + \theta)\,, \tag{1}$$

$$u(\theta) = u(\pi - \theta)\,. \tag{2}$$

Expression (1) ensures that the switched waveform has half-wave symmetry, i.e., its second half is equal to the negative of its first half. This symmetry property implies that only half of the waveform (i.e., switching angles) needs to be computed. Since each pulse is uniquely described by two switching angles, (1) indicates that only q switching angles are required.

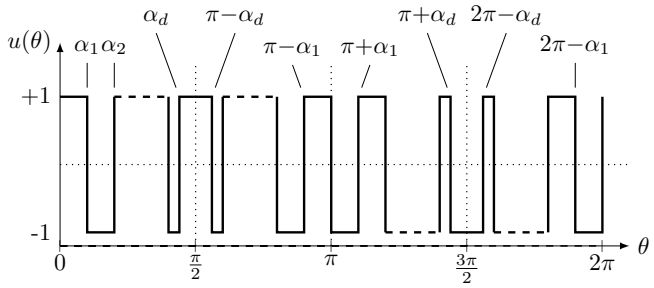

Fig. 2: Two-level "positive" ($u_0 = 1$) waveform with QaHWS.

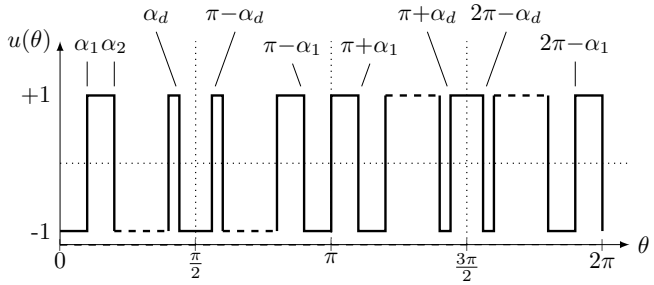

Fig. 3: Two-level "negative" ($u_0 = -1$) waveform with QaHWS.

Moreover, (2) imposes symmetry around $\pi/2$. This property further reduces the number of switching angles that need to be computed. Specifically, for a two-level converter, the number of to-be-computed switching angles is $d = (q-1)/2$, $d \in \mathbb{N}^+$ when QaHWS is imposed.[1]

Owing to the QaHWS properties, two different types of waveforms are introduced, namely one where the first switch position is $u_0 = 1$ (see Fig. 2), and one where $u_0 = -1$ (see Fig. 3). The Fourier representation of these pulse patterns is

$$u(\theta) = a_0 + \sum_{n=1}^{\infty} \left(a_n \cos(n\theta) + b_n \sin(n\theta)\right)\,. \tag{3}$$

where n is the harmonic order. Due to the QaHWS, the Fourier coefficients α_0 and α_n are zero, while b_n is

$$b_n = \begin{cases} u_0 \frac{4}{n\pi}\left(1 + 2\sum_{i=1}^{d}(-1)^i \cos(n\alpha_i)\right), & n = 1, 3, 5, \ldots \\ 0, & n = 2, 4, 6, \ldots \end{cases} \tag{4}$$

As a result, the amplitude of the $n^{\rm th}$ harmonic $\hat{u}_n$ of the pulse pattern u is given by

$$\hat{u}_n = u_0 \frac{4}{n\pi}\left(1 + 2\sum_{i=1}^{d}(-1)^i \cos(n\alpha_i)\right)\,. \tag{5}$$

With (5), the amplitude of the $n^{\rm th}$ voltage harmonic can be easily computed by considering the dc-link voltage, i.e.,

$$\hat{v}_n = \frac{V_{\rm dc}}{2}\hat{u}_n. \tag{6}$$

[1]Note that a fixed switching angle at π is imposed when considering two-level converters [3].

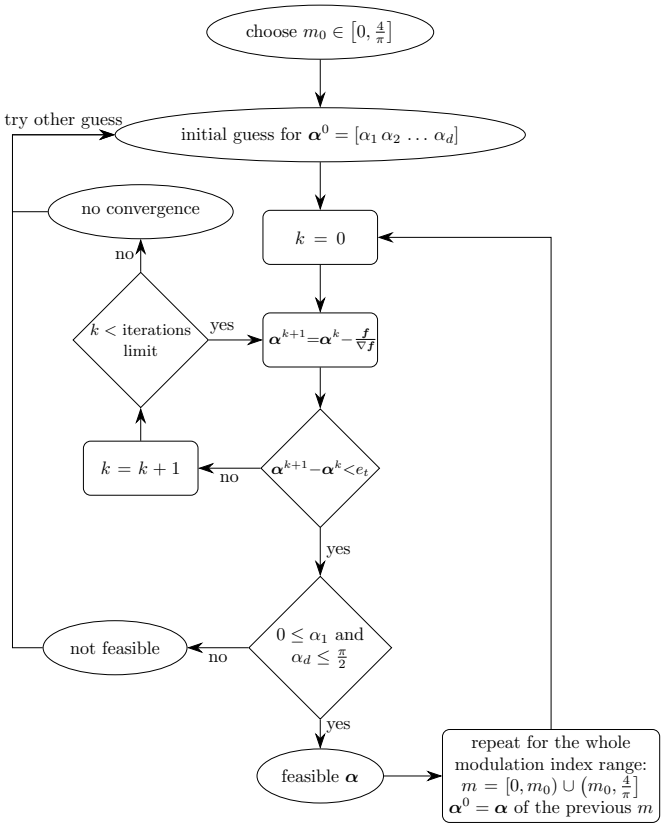

Fig. 4: SHE calculation algorithm based on the Newton-Raphson method.

A. Selective Harmonic Elimination

According to SHE, specific harmonics can be eliminated from the converter output voltage, by appropriately computing the switching angles of the applied pulse pattern. For q number of pulses per fundamental period, d harmonics can be controlled. Thus, $d-1$ harmonics can be completely eliminated, while the synthesis of the desired modulation index m is also achieved [15, Chapter 6.7], [3, Chapter 9.2]. To do so, the following set of nonlinear equations needs to be solved

$$\begin{bmatrix} u_0 \frac{4}{\pi}\left(1+2\sum_{i=1}^{d}(-1)^i\cos(\alpha_i)\right) \\ u_0 \frac{4}{5\pi}\left(1+2\sum_{i=1}^{d}(-1)^i\cos(5\alpha_i)\right) \\ \vdots \\ u_0 \frac{4}{n\pi}\left(1+2\sum_{i=1}^{d}(-1)^i\cos(n\alpha_i)\right) \end{bmatrix} = \begin{bmatrix} m \\ 0 \\ \vdots \\ 0 \end{bmatrix}. \quad (7)$$

One approach to numerically solve (7) is the Newton-Raphson method [15, Chapter 6.7], [16]. The flowchart of this method is shown in Fig 4, where $\boldsymbol{\alpha} = [\alpha_1\ \alpha_2\ \dots\ \alpha_n]^T$ is the vector of the to-be-computed switching angles, and the vector $\boldsymbol{f}$ is given by

$$\boldsymbol{f} = \begin{bmatrix} u_0 \frac{4}{\pi}\left(1+2\sum_{i=1}^{d}(-1)^i\cos(\alpha_i)\right) - m \\ u_0 \frac{4}{5\pi}\left(1+2\sum_{i=1}^{d}(-1)^i\cos(5\alpha_i)\right) \\ \vdots \\ u_0 \frac{4}{n\pi}\left(1+2\sum_{i=1}^{d}(-1)^i\cos(n\alpha_i)\right) \end{bmatrix}. \quad (8)$$

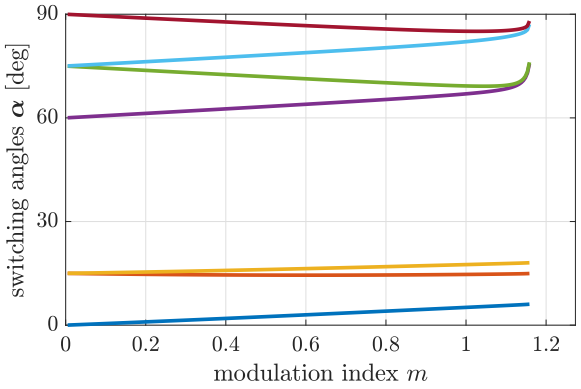

Fig. 5: SHE switching angles for $d = 7$.

Finally, e_t is the maximum accepted convergence tolerance (10^{-6} in this work), and k the iteration number.[2]

The problem is solved by choosing an initial modulation index m_0 and an initial guess of switching angles. To avoid potential inconsistency in the results, it is recommended to start solving the problem from a nonzero modulation index, i.e., $m_0 \neq 0$. Moreover, as the Newton-Raphson method is heavily depended on the initial guess [16], quasi-random Halton sequences are used to generate the initial points since they lead to better coverage—compared to a random sequence—of the search space. Subsequently, the results are filtered with MATLAB's command uniquetol, so that only unique solutions remain.

The number of angles d can be odd or even. When d is odd and $u_0 = 1$ (Fig. 2), a notch appears at the positive and negative peaks of the fundamental waveform, i.e., around the $90°$ and $270°$ of the fundamental. Similar behavior occurs when d is even and $u_0 = -1$, see Fig. 3. As this results in unacceptable solutions, typically, d must be even for the "positive" waveform ($u_0 = 1$), and odd for the "negative" waveform ($u_0 = -1$) [3, Chapter 9.2].

As mentioned, due to the nonlinear nature of the SHE problem, usually there are more than one feasible sets of angles for each problem. Moreover, the number of candidate solutions increases with the number of switching angles. As every set of solutions has different characteristics, some selection criteria should be defined. In some applications it is more useful to choose the set of angles that covers the widest range of modulation indices for higher utilization of the dc-link voltage. Nonetheless, in most applications, the best harmonic performance is the main objective, meaning that the most important criterion is to achieve the lowest possible current total demand distortion (TDD) I_{TDD}. As an example, Fig. 5 shows the SHE switching angles for $d = 7$ that result in the lowest I_{TDD}.

Finally, the computed switching angles $\boldsymbol{\alpha}$ for each pair $\{d, m\}$ are stored in a one-dimensional lookup table (LUT). The SHE angles can be retrieved in real time for control purposes depending on the desired operating point (i.e., mod-

[2]Note that a maximum limit of iterations is needed for non-converging angles (100 in this work) so that the algorithm always terminates.

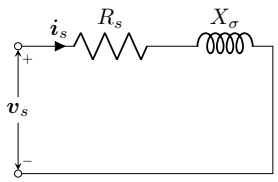

Fig. 6: Harmonic model of a machine.

ulation index m) and switching frequency (i.e., number of switching angles d).

B. Optimized Pulse Patterns

Stator currents with low harmonic distortions can result in lower iron and copper losses, and thus thermal losses, in the machine. Hence, programmed PWM patterns, i.e., OPPs, can be computed such that the current TDD is minimized. Given the nominal current $I_{s,\mathrm{nom}}$, the stator current TDD is defined as

$$I_{\mathrm{TDD}} = \frac{1}{\sqrt{2} I_{s,\mathrm{nom}}} \sqrt{\sum_{n \neq 1} \hat{i}_n^2}\,, \tag{9}$$

where $\hat{i}_n$ is the amplitude of the n^{th} current harmonic.

Consider the harmonic model of a machine in Fig. 6, where the reactances are lumped into the total leakage reactance X_σ. Assuming that the stator resistance R_s of the machine is very small (i.e., $R_s \approx 0$), the machine is a purely inductive load. Hence, $\hat{i}_n$ is given by

$$\hat{i}_n = \frac{\hat{v}_n}{n \omega_1 X_\sigma} = \frac{V_{\mathrm{dc}}}{2 \omega_1 X_\sigma} \frac{\hat{u}_n}{n}\,, \tag{10}$$

with ω_1 being the fundamental angular frequency. With (10), (9) becomes

$$I_{\mathrm{TDD}} = \underbrace{\frac{V_{\mathrm{dc}}}{2\sqrt{2} I_{s,\mathrm{nom}} \omega_1 X_\sigma}}_{\text{scaling factor}} \sqrt{\sum_{n \neq 1} \left(\frac{\hat{u}_n}{n} \right)^2}\,. \tag{11}$$

The first term (11) is a constant scaling factor, which depends on the converter and the load, but not on the pulse pattern. Hence, it can be neglected in the sequel as it does not affect the results of the optimization process. The second term accounts for the differential-mode voltage harmonics scaled by their harmonic order. By recalling (5), this term can be written as

$$J(\boldsymbol{\alpha}) = \sum_{n=5,7,\ldots} \frac{1}{n^4} \left(1 + 2 \sum_{i=1}^{d} (-1)^i \cos(n \alpha_i) \right)^2\,. \tag{12}$$

Expression (12) serves as the objective function for the OPP optimization problem. This is formulated as

$$\underset{\boldsymbol{\alpha} \in \left[0, \frac{\pi}{2}\right]^d}{\text{minimize}} \quad \sum_{n=5,7,\ldots} \frac{1}{n^4} \left(1 + 2 \sum_{i=1}^{d} (-1)^i \cos(n \alpha_i) \right)^2 \tag{13}$$

$$\text{subject to} \quad u_0 \frac{4}{\pi} \left(1 + 2 \sum_{i=1}^{d} (-1)^i \cos(\alpha_i) \right) = m \tag{14}$$

$$0 \leq \alpha_1 \leq \alpha_2 \leq \cdots \leq \alpha_d \leq \frac{\pi}{2}\,. \tag{15}$$

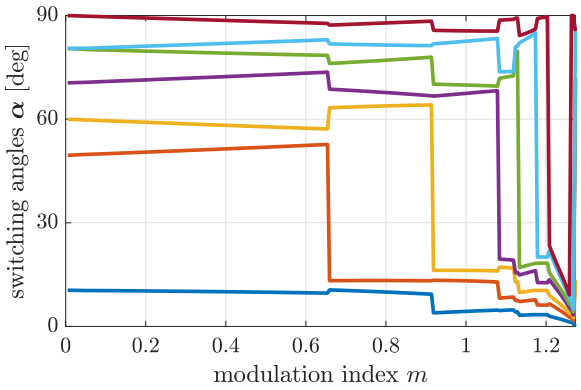

Fig. 7: OPP switching angles for $d = 7$.

TABLE I: Rated values of the drive system

Parameter	Symbol	Value
nominal stator current	I_N	535 A
nominal power	P_N	144 kW
nominal torque	T_N	393 Nm
nominal speed	n_N	3500 rpm
dc-link voltage	V_{dc}	325 V

TABLE II: Operating points

	f_1 [Hz]	operation	i_d [A]	i_q [A]
1.	400	motor	−85	40
2.	400	generator	−85	−40
3.	475	motor	−10	10
4.	475	generator	−10	−10

In the above optimization problem, the equality constraint (14) guarantees that the desired modulation index $m \in [0, 4/\pi]$ is synthesized. Moreover, the inequality constraints (15) ensure that the optimized angles are in ascending order and within the interval $[0, \pi/2]$ due to the QaHWS of the OPP.

As the OPP optimization problem is nonconvex, multiple local minima exist. This makes the solution process extremely time consuming. In this work, the MATLAB optimization toolbox is utilized, while, similar to SHE, Halton sequences are used to generate the initial guesses. Finally, it is worth mentioning that the OPPs switching angles are stored in LUTs in the same fashion as the SHE angles, i.e., for each pair $\{d, m\}$. For visualization purposes, the QaHWS OPP switching angles for $d = 7$ are shown in Fig. 7.

III. Performance Evaluation

The synchronous PWM techniques described in Section II are experimentally assessed with a drive train used in electric vehicles. The nominal values of the IPMSM and two-level inverter are summarized in Table I. FOC is used to manipulate the SHE- and OPP-based pulse patterns. Finally, asynchronous SVM is used as a benchmark modulation strategy.

Four operating points in the lower-torque range are chosen at two different speeds (i.e., fundamental frequencies f_1), see Table II. That is because the electric drive trains usually operate in that region, while the higher-torque range is used only in acceleration/deceleration for small time intervals. The

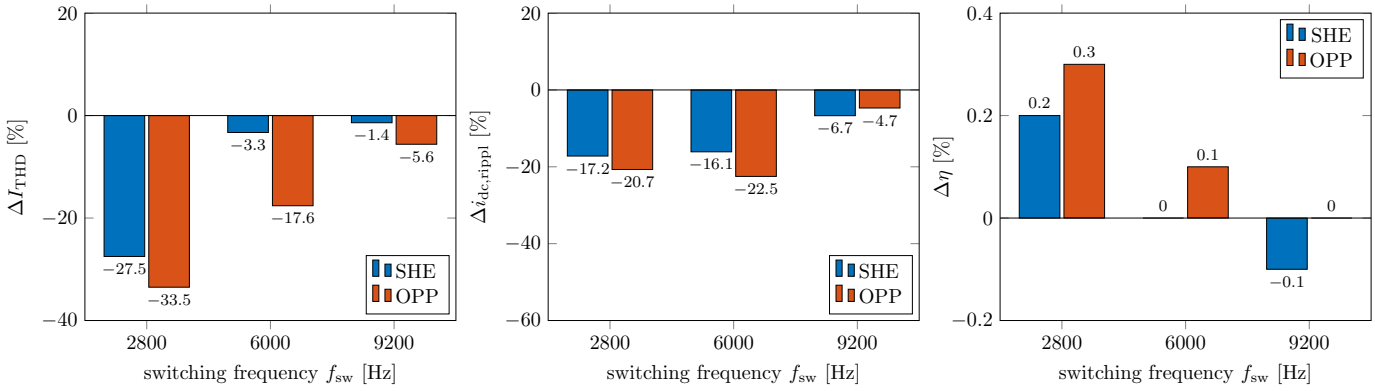

Fig. 8: Experimental results for motor operation at $f_1 = 400\,\mathrm{Hz}$, $i_d = -85\,\mathrm{A}$, $i_q = 40\,\mathrm{A}$.

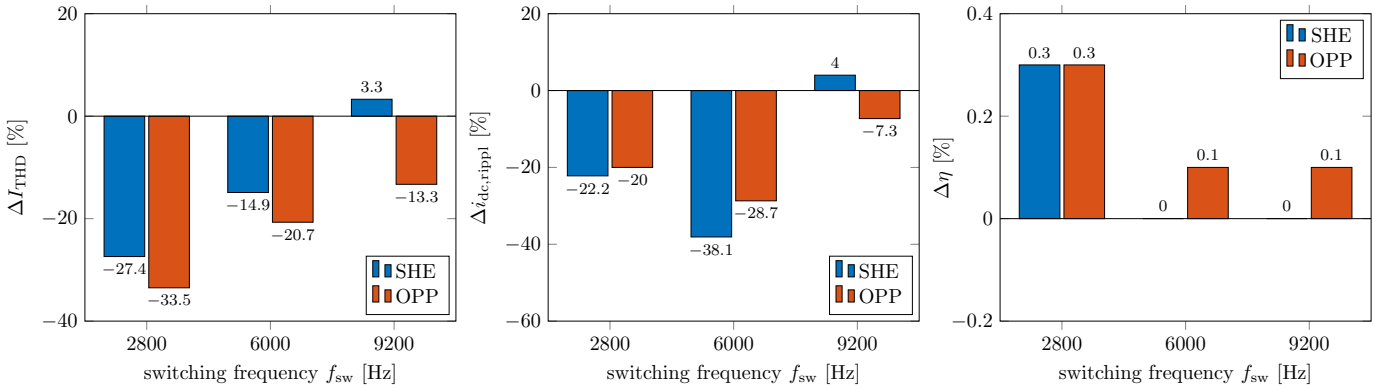

Fig. 9: Experimental results for generator operation at $f_1 = 400\,\mathrm{Hz}$, $i_d = -85\,\mathrm{A}$, $i_q = -40\,\mathrm{A}$.

PMSM is operated not only as a motor, but also as a generator to examine the performance of the modulation schemes in regenerative braking. Three different switching frequencies are tested at each operating point, implying SHE sets and OPPs of three different values of d, namely $d = 3$, 7, and 11, and SVM with switching frequency $f_{\mathrm{sw}} = (2d{+}1)f_1$. At every switching frequency, the stator current total harmonic distortion (THD) I_{THD}, the electric drive system efficiency η (i.e., percentage of dc input power converted to mechanical output power), and the current ripple at the dc link $i_{\mathrm{dc,rippl}}$ are measured. The results obtained with asynchronous SVM are used as reference for each operating point. For demonstration purposes (see Figs. 8 to 11), the relative difference between the SVM and synchronous modulation results serves as a performance metric, i.e.,

$$\Delta\xi = \frac{\xi_\sigma - \xi_{\mathrm{SVM}}}{\xi_{\mathrm{SVM}}} \cdot 100\%, \tag{16}$$

where ξ stands either for I_{THD}, efficiency η, or dc-link current ripple $i_{\mathrm{dc,rippl}}$, while σ indicates the synchronous PWM scheme, i.e., OPPs or SHE.

As can be seen in Figs. 8 to 11, the I_{THD} results confirm the superiority of the synchronous PWM schemes, especially at the lower switching frequencies. Specifically, OPPs produce the lowest I_{THD} in all examined cases, thus clearly outperforming SVM and SHE. As for SHE, even though in most cases it outperforms SVM, the I_{THD} improvement becomes smaller as the switching frequency increases, while in one case ($f_{\mathrm{sw}} = 9200\,\mathrm{Hz}$ in Fig. 9) SVM achieves better results.

The dc-link current ripple of the synchronous modulation schemes is significantly lower than that with SVM when operating at low load, i.e., $i_d = -10\,\mathrm{A}$ and $i_q = \pm 10\,\mathrm{A}$, see Figs. 10 and 11. At a higher load ($i_d = -85\,\mathrm{A}$ and $i_q = \pm 40\,\mathrm{A}$), a smaller ripple mitigation can be observed, while as the switching frequency increases the reduction of the dc-link current ripple becomes smaller. In motor mode, OPPs are clearly the best solution. However, in generator mode, SHE can offer similar, if not bigger, reduction, see Figs. 9 and 11.

Finally, regarding the drive system efficiency, similar to I_{THD}, OPPs operate the drive at the highest efficiency in all operating points and switching frequencies in question. As a result, the efficiency improvement attributed to OPPs can be as high as 2.7% compared with SVM in motor mode, see Fig. 10, and 3.6% in generator mode, see Fig. 11. Nevertheless, when the ratio between the switching and fundamental frequency is relatively high the advantage of OPPs is smaller, whereas in one case the efficiency remains the same as with SVM. Similarly, SHE can reach up to 3.2% improved efficiency at low switching-to-fundamental frequency ratios. However, as the ratio increases, SVM achieves the same or higher efficiency than SHE. Hence, based on the presented results, it can be concluded that the benefits of synchronous modulation are prevalent when the ratio between the switching and fundamental frequency is small.

IV. Conclusions

In this paper, three different modulation techniques for electric automotive vehicles—namely synchronous modulation

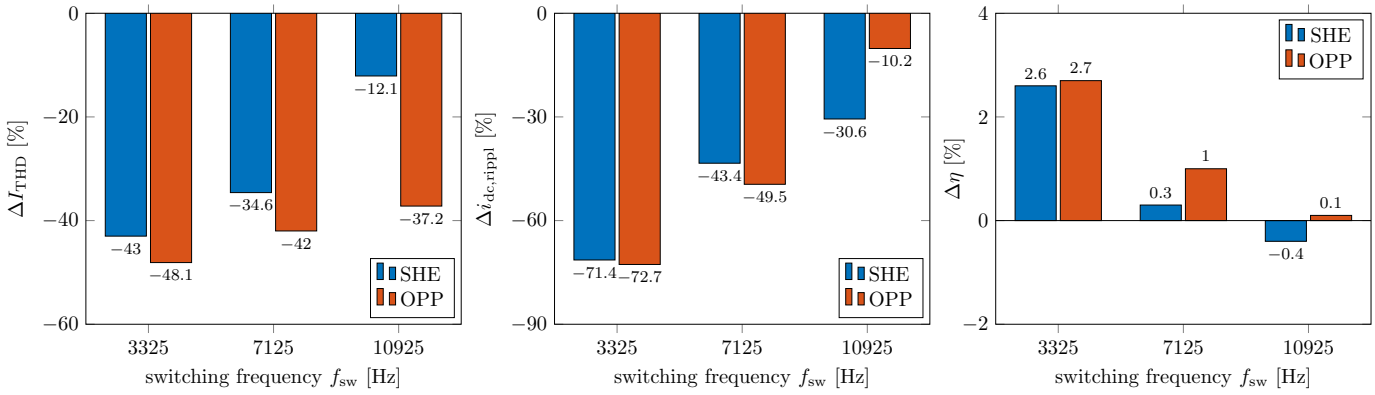

Fig. 10: Experimental results for motor operation at $f_1 = 475\,\mathrm{Hz}$, $i_d = -10\,\mathrm{A}$, $i_q = 10\,\mathrm{A}$.

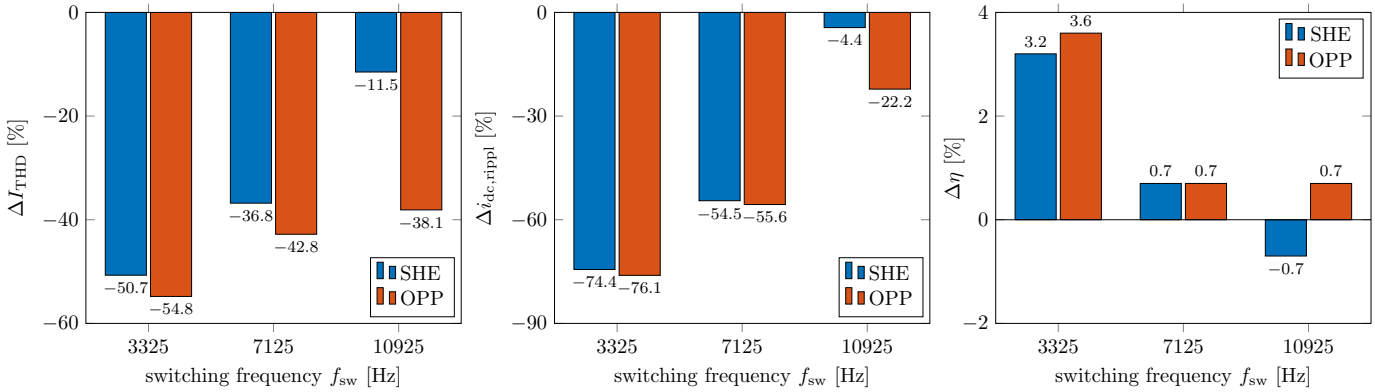

Fig. 11: Experimental results for generator operation at $f_1 = 475\,\mathrm{Hz}$, $i_d = -10\,\mathrm{A}$, $i_q = -10\,\mathrm{A}$.

in the form of SHE and OPPs as well as asynchronous SVM—were experimentally assessed. The presented results demonstrated the advantages of synchronous PWM schemes in the lower-torque range. Specifically, OPPs can achieve the overall best performance at all operating points and switching frequencies in terms of current distortions, system efficiency and dc-link current ripple. Hence, thanks to OPPs, both the power converter and machine can be operated under less stress, thus improving their lifetime and decreasing the maintenance requirements. As shown in this paper, it can be concluded that synchronous modulation methods, and especially OPPs, constitute a relevant modulation strategy for drive trains used in automotive applications.

References

[1] M. Ehsani, K. V. Singh, H. O. Bansal, and R. T. Mehrjardi, "State of the art and trends in electric and hybrid electric vehicles," *Proc. IEEE*, vol. 109, no. 6, pp. 967–984, Jun. 2021.

[2] M. L. De Klerk and A. K. Saha, "A comprehensive review of advanced traction motor control techniques suitable for electric vehicle applications," *IEEE Access*, vol. 9, pp. 125 080–125 108, Sep. 2021.

[3] D. G. Holmes and T. A. Lipo, *Pulse Width Modulation for Power Converters: Principles and Practice*. Piscataway, NJ, USA: John Wiley and Sons, 2003.

[4] J. Holtz, "Pulsewidth modulation—A survey," *IEEE Trans. Ind. Electron.*, vol. 39, no. 5, pp. 410–420, Oct. 1992.

[5] M. S. A. Dahidah, G. Konstantinou, and V. G. Agelidis, "A review of multilevel selective harmonic elimination PWM: Formulations, solving algorithms, implementation and applications," *IEEE Trans. Power Electron.*, vol. 30, no. 8, pp. 4091–4106, Aug. 2015.

[6] H. S. Patel and R. G. Hoft, "Generalized techniques of harmonic elimination and voltage control in thyristor inverters: Part I—Harmonic elimination," *IEEE Trans. Ind. Appl.*, vol. IA-9, no. 3, pp. 310–317, May 1973.

[7] ——, "Generalized techniques of harmonic elimination and voltage control in thyristor inverters: Part II—Voltage control techniques," *IEEE Trans. Ind. Appl.*, vol. IA-10, no. 5, pp. 666–673, Sep. 1974.

[8] G. S. Buja and G. B. Indri, "Optimal pulsewidth modulation for feeding ac motors," *IEEE Trans. Ind. Appl.*, vol. IA-13, no. 1, pp. 38–44, Jan. 1977.

[9] A. Birth, T. Geyer, H. d. T. Mouton, and M. Dorfling, "Generalized three-level optimal pulse patterns with lower harmonic distortion," *IEEE Trans. Power Electron.*, vol. 35, no. 6, pp. 5741–5752, Jun. 2020.

[10] B. K. Bose and H. A. Sutherland, "A high-performance pulsewidth modulator for an inverter-fed drive system using a microcomputer," *IEEE Trans. Ind. Appl.*, vol. IA-19, no. 2, pp. 235–243, Mar. 1983.

[11] D. Horstmann and G. Stanke, "Die stromrichternahe Antriebsregelung des Steuergerates für Bahnautomatisierungssysteme SIBAS 32," SIEMENS, Tech. Rep., Jan. 1992.

[12] K. Douzane, L. Rinehart, C. Keraudren, S. Rodhain, and F. Tahiri, "Inverter and motor efficiency increase with FPCU implementing optimized pulse pattern methods," in *Proc. Int. Electr. Vehicle Symp. and Exhib.*, Nanjing, Jiangsu, Jun. 2021, pp. 1–12.

[13] R. Klink, D. Heintges, S. Aleff, R. Scheer, and J. Andert, "DENSO's novel development strategy for power electronics and controllers," in *Proc. Aachen Coll. Sustain. Mobil.*, Aachen, Germany, Oct. 2021, pp. 1–14.

[14] A. Birda, J. Reuss, and C. M. Hackl, "Simple fundamental current estimation and smooth transition between synchronous optimal PWM and asynchronous SVM," *IEEE Trans. Ind. Electron.*, vol. 67, no. 8, pp. 6354–6364, Aug. 2020.

[15] S. N. Manias, *Power Electronics and Motor Drive Systems*. Cambridge, MA, USA: Academic Press, 2016.

[16] V. G. Agelidis, A. I. Balouktsis, and C. Cossar, "On attaining the multiple solutions of selective harmonic elimination PWM three-level waveforms through function minimization," *IEEE Trans. Ind. Electron.*, vol. 55, no. 3, pp. 996–1004, Mar. 2008.